Available online at www.sciencedirect.com
ScienceDirect
Journal of the European Ceramic Society 31 (2011) 2923–2929
www.elsevier.com/locate/jeurceramsoc

Effect of substrate temperature on the microstructure and properties of thick plasma-sprayed YSZ TBCs

S.A. Tsipas [a,*], I.O. Golosnoy [b,c]

[a] Department of Materials Science and Engineering, IAAB, University Carlos III of Madrid. Avda. Universidad 30, 28911 Leganés, Spain
[b] Electrical Power Engineering Research Group, School of Electronics and Computer Science, University of Southampton, Southampton, UK

Received 4 April 2011; received in revised form 13 July 2011; accepted 21 July 2011
Available online 15 August 2011

Abstract

Thick (~1.2 mm) thermal barrier coatings (TBCs) consisting of YSZ were deposited by plasma spraying. Spraying parameters were varied in a controlled manner to produce different microstructures. The effect of substrate temperature on the microstructural features and subsequently on the Young's modulus was investigated. In addition, the residual stresses in the coatings were estimated using a numerical model and they were related to the microstructural features observed. Results showed that crack segmentation density, residual stresses in the coatings and thus coating properties are strongly affected not only by the average substrate temperature during spraying but also the variations between the minimum and maximum substrate temperature.

Keywords: Porosity; ZrO_2; Residual stress; Microstructure; Thermal barrier coatings

1. Introduction

Further efficiency improvements in turbine technology for aero engines as well as land-based gas turbines require increased operating temperatures. However, limits on the operating temperature are imposed by the onset of melting of the superalloys. TBCs offer benefits in terms of the performance and efficiency of gas turbines, allowing lower metal temperatures, reduced requirements for active cooling, higher turbine entry temperatures and longer component lifetimes. TBC systems are composed of a zirconia ceramic top coat (300–600 μm thick), over a metallic bond coat (100 μm thick). The industry standard material used as a top coat is zirconia, usually stabilised with 7–8 wt.% yttria. The top coat (TC) acts as a thermal barrier, generating a temperature drop of up to ~300 °C, while the bond coat (BC) provides corrosion and oxidation protection for the substrate and creates a rough surface which may promote adhesion of the top coat. The top coat is deposited either by electron beam assisted physical vapour deposition (EB-PVD) or air plasma spraying (APS).

Failure of TBCs usually occurs by buckling and spalling of the coating. APS top coats, which are considerably cheaper to produce, are composed of overlapping splats oriented parallel to the plane of the coating, with poor inter-splat bonding, many microcracks and pores. Therefore, they have very low stiffness. This prevents large stresses, and hence large driving forces for spallation, from being generated in the top coat. Thick thermal barrier coatings provide greater temperature drops across the coating, which offers advantages with respect to reduction of the cooling air required by hot components or allows increases in gas turbine inlet temperature, thus increasing the efficiency and performance of the engine.[c] It is calculated that the use of 1.5 mm thick TBCs instead of the current ones could reduce the amount of cooling required by the hot component (combustion chamber liner) up to 60% of the present value while maintaining the same metal temperature.[2] However thick TBCs show low thermal shock resistance.[1,3] With increased thickness, the elastic strain energy stored in the coating increases and hence the driving force for spallation increases. Microstructural modifications that induce microcracks, segmentation cracks and porosity can increase the thermal shock resistance of thick TBCs.[4–7]

* Corresponding author. Tel.: +34 916248374; fax: +34 916249430.
E-mail addresses: stsipas@ing.uc3m.es, sofia.tsipas@quim.ucm.es (S.A. Tsipas), i.golosnoy@soton.ac.uk (I.O. Golosnoy).
[c] Tel.: +44 2380597694; fax: +442 380593709.

0955-2219/$ – see front matter © 2011 Elsevier Ltd. All rights reserved.
doi:10.1016/j.jeurceramsoc.2011.07.022

The scope of this work is to successfully deposit thick TBCs and investigate how processing parameters can be related to the microstructural features that will increase the thermal shock resistance of thick TBCs. Not only is the effect of substrate temperature on the microstructural features established, but also the mechanisms of generation of these features is related to residual stresses in the coatings, which are estimated using a model. The microstructural features are then related to the mechanical properties of the coatings.

2. Experimental procedure

The powders were supplied by Sulzer-Metco (US) Inc. The bond coat material, designated Amdry 995/C, has a nominal composition (in wt.%) of Co–32Ni–21Cr–8Al–0.5Y. The top coat was yttria partially stabilised zirconia (YPSZ) (ZrO_2-7.6 wt.%Y_2O_3), designated 204NS-1. These were deposited onto mild steel substrates of thickness of 1 mm. The choice of the substrate material was made to simplify the de-bonding of the coatings from the substrate after spraying without compromising the thermal and elastic properties. Mild steels and nickel superalloys have similar coefficients of thermal expansion and the level of residual stresses is expected to be similar for both substrates. Also for typical spraying conditions substrate temperatures are several hundred degrees and the thermal conductivities are actually similar for both substrate materials at these temperatures. Specimens were produced by vacuum plasma spraying of the bond coat, followed by air plasma spraying of the top coat. Spraying was carried out the Department of Materials Science and Metallurgy at the University of Cambridge. Details of the spraying conditions can be found elsewhere.[8] Gun motion during spraying in the *x*–*y* plane was programmed using a raster pattern as the one shown in Fig. 1. The raster pattern was repeated for a number of cycles. The substrate temperature was varied by cooling the back surface of the substrate during spraying with a jet of compressed air and/or by waiting 35 s in-between each gun pass. The substrate temperature during deposition was monitored by a thermocouple attached to the backsurface of the substrate. Coatings with thicknesses of about 1.2 mm were produced.

Coatings sprayed at four different average substrate temperatures were examined. The four samples have been labelled as A (produced by continuous spraying), B (produced by waiting between gun cycles), C (produced by continuous spraying with forced air cooling of the substrate) and D (produced by waiting between gun cycles with forced air cooling of the substrate). The average substrate temperature decreases from A to D.

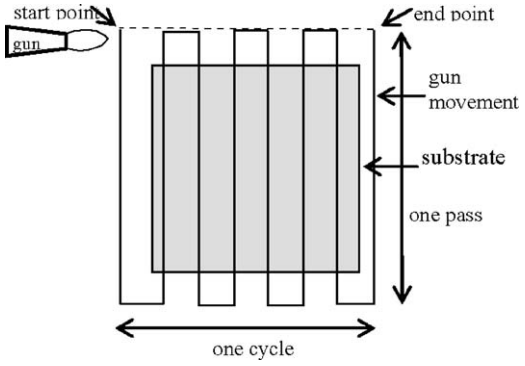

Fig. 1. Raster pattern in the *x*–*y* plane for one cycle of gun movement.

The sprayed specimens were vacuum impregnated with epoxy. Struers Epovac vacuum impregnation equipment and Struers Caldofix epoxy were used. The specimens were ground and finely polished to a 1 μm diamond finish. Cross sections of the samples were examined by optical microscopy. The microstructural features observed have been defined as follows: (i) segmentation cracks (cracks running perpendicular to the coating surface and penetrating at least half the coating thickness), (ii) branching cracks (cracks parallel to the coating plane, starting from segmentation cracks), (iii) microcracks (other cracks in the coating not fulfilling the criteria of segmentation or branching cracks) and (iv) porosity (spherical porosity in the cross section of the coating). The segmentation crack density was calculated by dividing the number of segmentation cracks present in each cross section by the cross section length.

Stiffness measurements were made using cantilever bending. Details of the cantilever bend testing are given elsewhere.[9] A model developed by Clyne and co-workers[10–13] was used in the present work for the prediction of residual stresses. The model predicts the temperature, curvature and stress distribution through the coating and substrate during the plasma spraying deposition process.

3. Results and discussion

The average backsurface temperature during spraying for the coatings deposited is shown in Fig. 2. The cross-sections of the detached plasma sprayed coatings that were produced varying the substrate temperature are shown in Figs. 3–6. The tempera-

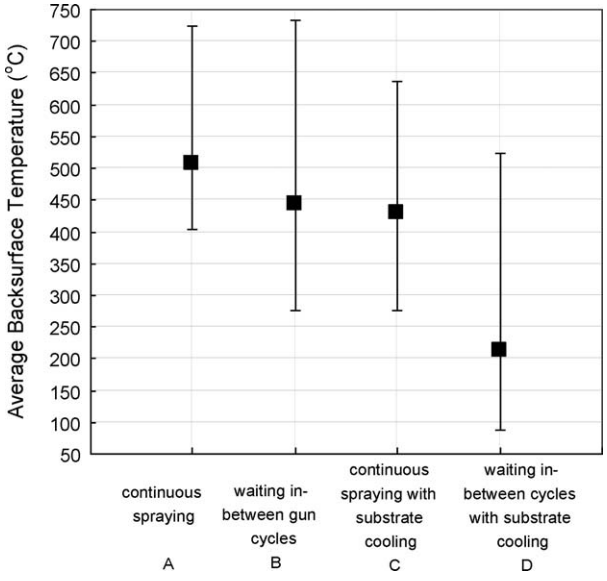

Fig. 2. Average substrate back-surface temperature (T_{av}) during spraying of YPSZ-TC for different cooling conditions. The vertical bars indicate the temperature range of the substrate during spraying.

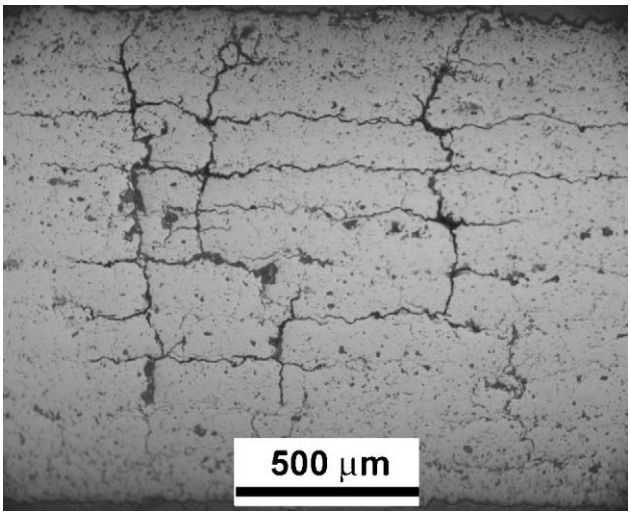

Fig. 3. Polished cross section of coating A [T_{av} = 507 °C].

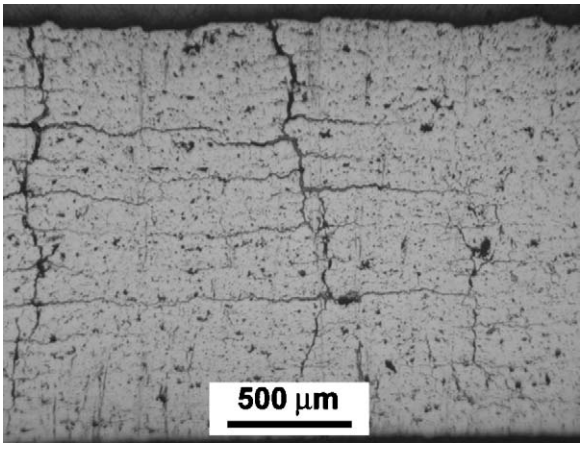

Fig. 4. Polished cross section of coating B [T_{av} = 445 °C].

ture of the substrate changes continuously during spraying, due to the movement of the spraying gun. The average backsurface temperature is calculated by considering the temperature distribution during spraying and considering the time at temperature.

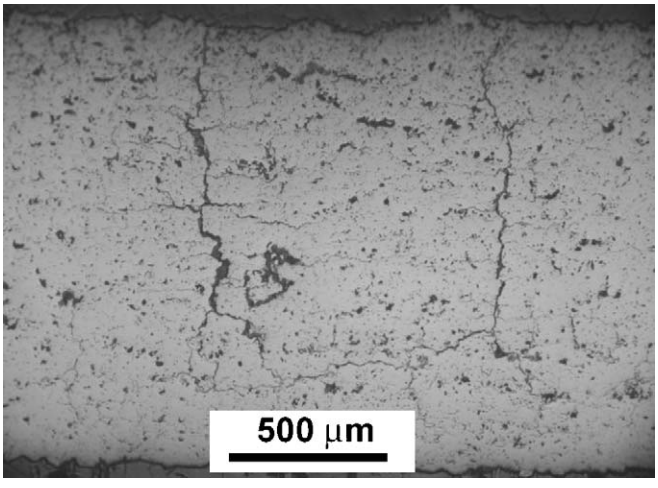

Fig. 5. Polished cross section of coating C [T_{av} = 429 °C].

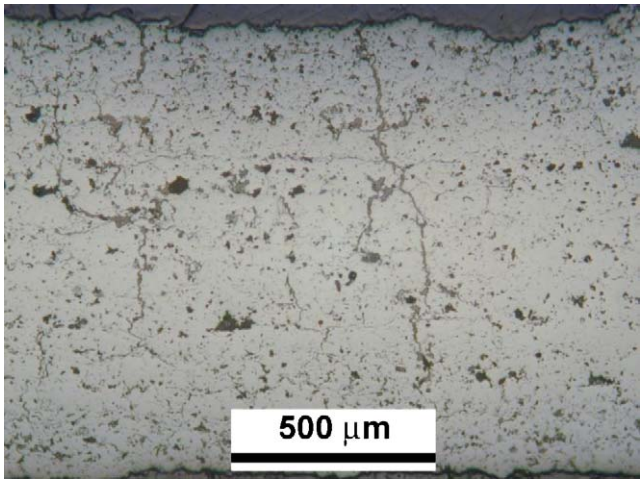

Fig. 6. Polished cross section of coating D [T_{av} = 212 °C].

In addition to the average temperature, the vertical bars in Fig. 2 indicate the maximum and minimum temperatures of the backsurface of the substrate during spraying. It can be seen that the variation of the backsurface temperature is very large for all coatings, in some cases as high as 450 °C. This is expected to be significant for the generation of the microstructure of the sprayed coatings. It is also important to note that the temperatures measured are at the back surface and much higher temperatures are experienced where coating deposition occurs.

The density of segmentation cracks was measured in all coatings. Coating A, which was sprayed with the highest average backsurface temperature, had the highest levels of segmentation cracks (1.1 mm^{-1}), as well as significant branching cracks originating from them. Coating D, had the lowest average back surface temperature, as a result of cooling the substrate during spraying and waiting in-between gun cycles. This coating had a segmentation crack density of 0.7 mm^{-1} and no branching cracks were present. Coatings B and C had a similar average backsurface temperatures during spraying. Nevertheless, the difference between the minimum and maximum temperatures in coating B was about 100 °C more than in coating C. In coating B, where there was a higher difference between maximum and minimum temperature, the crack segmentation density is relatively low (0.72 mm^{-1}) and there are no branching cracks present. Coating C, where lower differences exist between the maximum and minimum temperature, has a higher segmentation crack density (of 0.91 mm^{-1}) and very few branching cracks.

These observations suggest that both the average substrate temperature and the range of temperatures (maximum and minimum) during deposition are important and that higher average substrate temperatures and lower differences between the maximum and minimum substrate temperature seem to give rise to coatings with higher density of segmentation cracks.

In order to understand the mechanism for the development of these segmentation cracks, it is necessary to examine in detail the evolution of the temperature changes in the coating during spraying and the residual stresses generated as a consequence of these temperature changes. The backsurface temperature patterns is shown in Figs. 7–10 indicate that there is a marked temperature

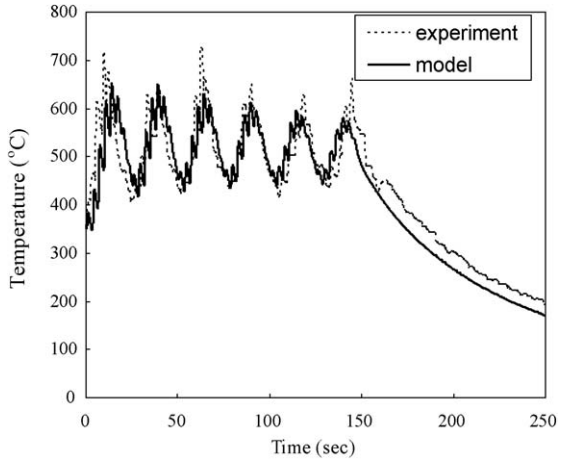

Fig. 7. Experimental and modelled back surface thermal histories for coating A [T_{av} = 507 °C].

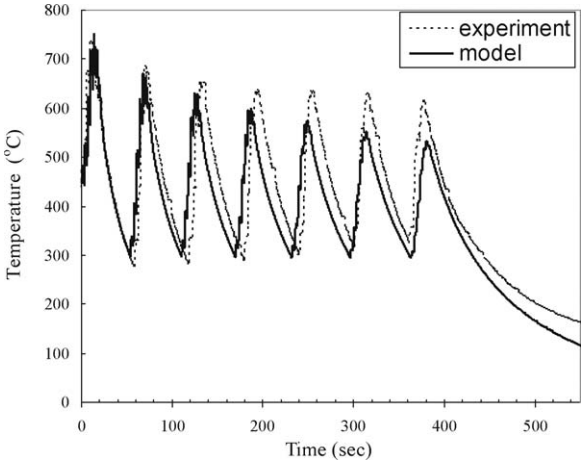

Fig. 8. Experimental and modelled back surface thermal histories for coating B [T_{av} = 445 °C].

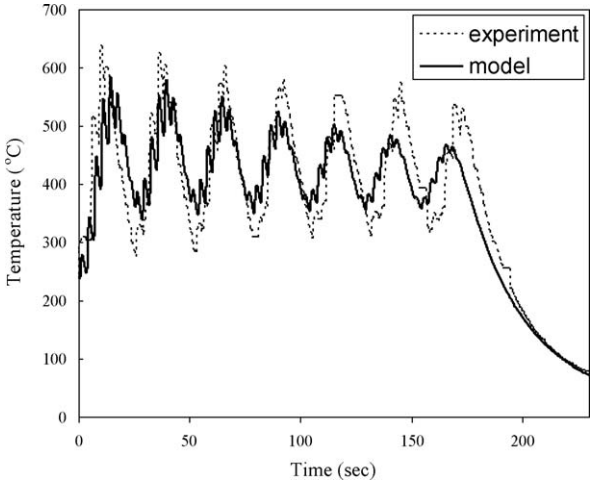

Fig. 9. Experimental and modelled back surface thermal histories for coating C [T_{av} = 429 °C].

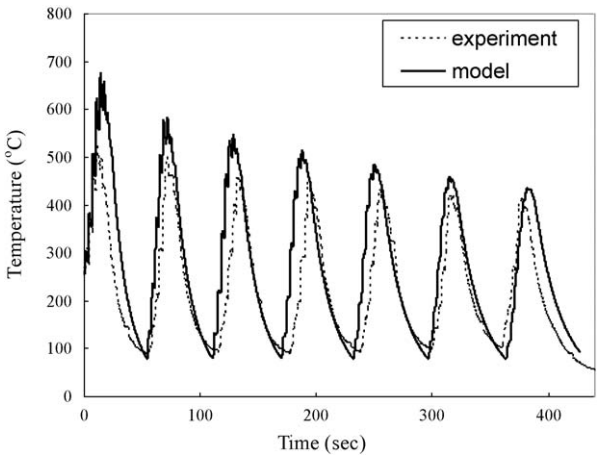

Fig. 10. Experimental and modelled back surface thermal histories for coating D [T_{av} = 212 °C].

drop in-between gun cycles, once the spraying gun has completed the raster pattern and before it initiates the next one. This temperature drop is more pronounced when compressed air is applied at the backsurface of the coating (coatings B and D) and/or when waiting 35 s in-between each gun cycle (C and D). It has been suggested that at high average substrate temperature there will be improved contact between splats.[14–16] Hence, it is possible that weak interfaces where poor splat bonding exists are formed in-between gun cycles due to the drop in temperature that the coating experiences.

A possible mechanism for the generation of segmentation cracks is that they are created when the sample is cooled to room temperature, after the deposition process is complete, as a result of relaxation of bi-axial stresses.[17] The segmentation crack is initiated at the free surface and propagates through the thickness of the coating. As it propagates is reaches the weak interfaces between layers where poor splat bonding exists. These layers can be formed in-between gun cycles, once the spraying gun has completed the raster pattern and initiates the next one. When a segmentation crack reaches the weak interfaces that exist in-between these layers, the stresses at the crack tips can be relieved by opening up branching cracks. High average substrate temperature favours improved contact between splats,[14,15] and hence it is probable that due to this improved contact between splats stresses in the top coat cannot relax by generation of branching cracks in-between layers or splats. Thus in coatings with high average substrate temperature and low difference between minimum and maximum temperature relaxation occurs by the generation of segmentation cracks and few branching cracks are present. Also when the difference between the minimum and maximum spraying temperature is high, even if the average substrate temperature is high, bonding between splats is poor and hence stresses can relax by generation of microcrakcs and/or branching cracks and the segmentation crack density is relatively low. Similar results have been observed by other researchers.[4,18,19]

The numerical model developed by Clyne and coworkers[10,11,13,20,21] was used to calculate the stresses in the top coat and get further insight into other possible mechanisms

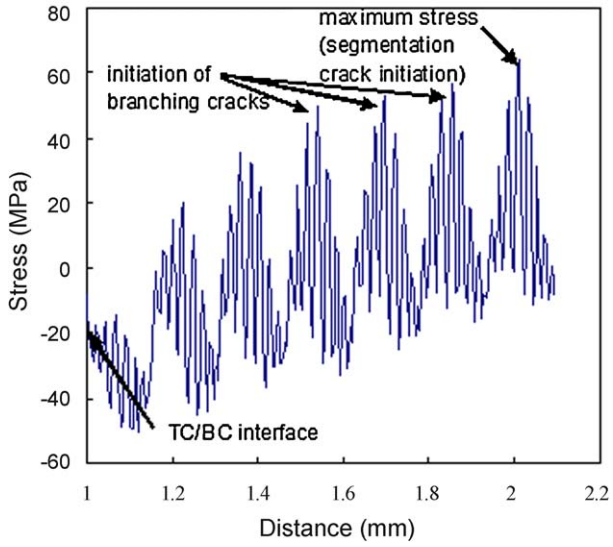

Fig. 11. Residual stress through thickness of as-sprayed YPSZ-TC sprayed by waiting in-between each gun cycle (B).

for the generation of the segmentation and branching cracks. The measured thermal history was compared to that obtained using the numerical model. Comparisons of experimental and modelled backsurface thermal histories for each of the different spraying conditions are shown in Figs. 7–10. The agreement for all cases is good. The residual stress distribution through the coating at different stages of the spraying process was then obtained from the numerical model. Fig. 11 shows the final residual stress distribution through the thickness of the coating B produced by waiting in-between each gun cycle. The rest of the coatings (A, C and D) show a similar final residual stress distribution. There is a stress gradient through the thickness of the coating, with compressive stresses at the TC/BC interface and tensile stresses in the outer surface. There is also a large variation in the stress range with periodic peaks of high tensile stress. This pattern is due to the movement of the spraying gun through the modelling point in every gun cycle. As the spraying gun moves towards the modelling point in each pass, the stress range gradually increases and then decreases when the gun moves away, resulting in a variation of the stress that the coating experiences. The point where the coating experiences the highest tensile stresses is near the outer surface. The results from the model suggest that near the free surface of the top coat there are high tensile stresses that could lead to initiation of the segmentation cracks. It is possible that branching cracks initiate from the segmentation cracks at places of weak splat bonding and where there are peaks of high tensile stress (see Fig. 4). It is worth noting that stresses change from compressive to tensile many times during the deposition and it is possible that this potentially causes initiation points for segmentation cracks and/or branching cracks.

Nevertheless it is necessary to examine other possible mechanisms for the generation of segmentation and branching cracks, by closely observing the temperature and stress distribution during spraying. As mentioned earlier the predicted final stress distribution in all samples (A, B, C and D) is similar and probably

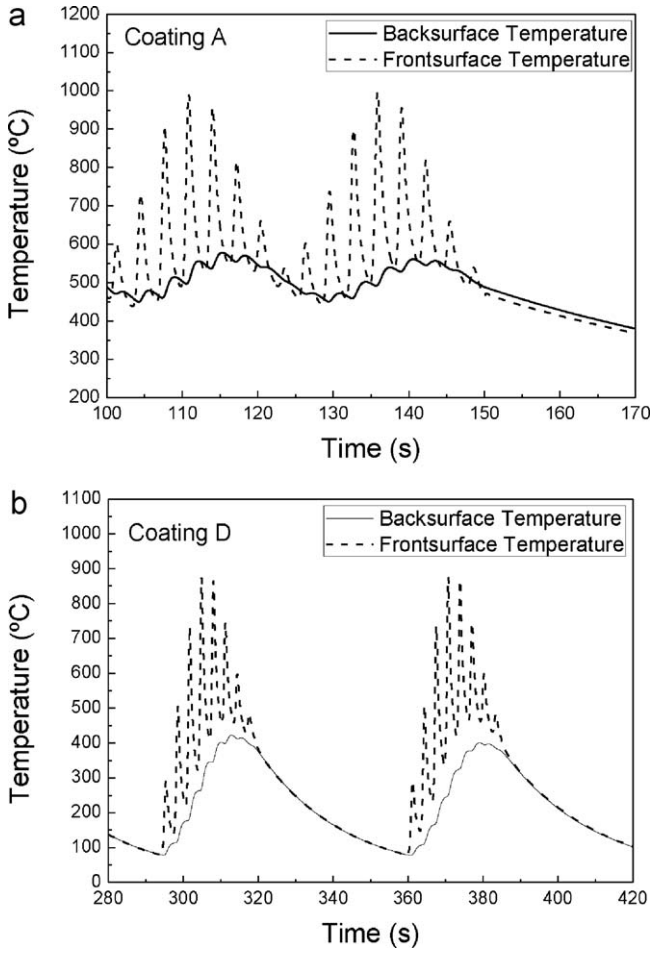

Fig. 12. Predicted back and front surface thermal histories for coatings (a) A and (b) D, respectively, during the last 2 gun passes.

cannot fully explain the observed differences in the segmentation crack densities. Fig. 12 shows the predicted front surface temperature for coatings A and D for the measured backsurface temperature. It can be seen that the temperature at any given point in the front surface of the coatings changes very rapidly, by a range as high as 500 °C as the gun moves back and forward about the modelling point in a single raster cycle and the temperature decreases in between gun cycles (for coating D). Such large changes in temperature are not surprising given the high temperature of the plasma.[22] It is possible that during these rapid temperature variations, the ceramic coating might experience complex stress states near the surface and subsequent weakening causing the generation of the segmentation cracks.

Fig. 13 shows the stress distribution along the thickness of coating A at different times during the deposition process. Specifically the stress distribution in the coating for time instances where the temperature difference between the front and back surface is minimum (such as in-between gun cycles) is compared to the stress in the coating for time instances where there is a maximum temperature drop along the coating thickness (the gun position is close to the modelling point). As it can be seen, the predicted stress magnitudes are similar during these stages of deposition, except near the outer surface where more

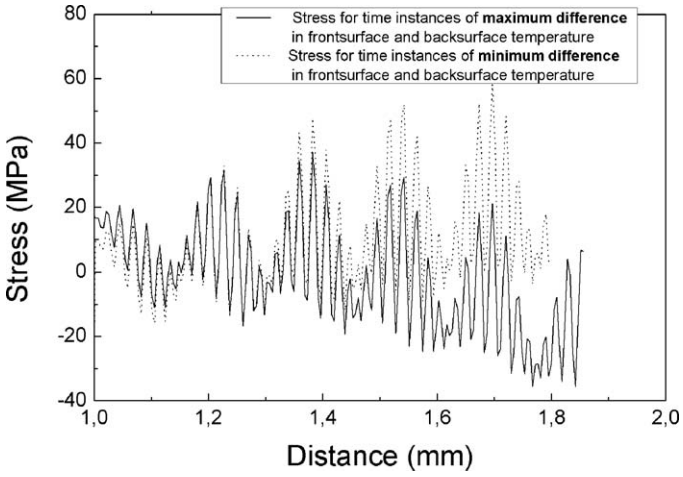

Fig. 13. Thermal stress through thickness of as-sprayed YPSZ-TC during different stages of the process.

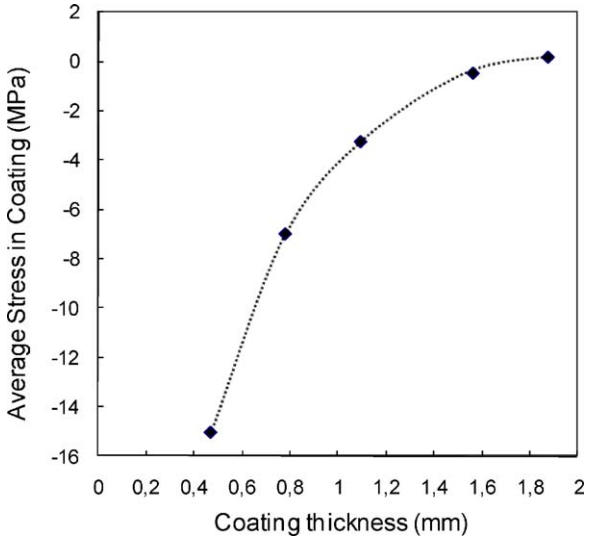

Fig. 14. Average residual stress in APS-YPSZ top coats of different thickness.

pronounced differences are observed. The same is true for all coatings (A, B, C, and D) where the stress magnitudes are similar during the various stages of deposition. However there are significant differences between the front surface temperatures that the coatings experience during deposition. For example, the surface temperature for A is approximately 100 degrees higher than the one for D (Fig. 12). Exact properties of YPSZ are not known at such high temperatures, but we can expect a significant weakening of coating A in comparison to D. This suggests that the weakening of coatings at high temperature probably plays a significant role in formation segmentation cracks.

Segmentation and branching cracks are characteristic of thick TBCs and are not present in coatings less than about 1 mm thick. The average stress state in the top coat after spraying coatings of different thickness was estimated using the numerical model by matching the measured and modelled thermal histories. The error associated to the stress values will depend on details of the substrate properties (coefficient of thermal expansion and yield stress as a function of temperature). The results show that the average residual stress in the top coat changes from compressive to tensile with increasing coating thickness (see Fig. 14). For thick coatings the average residual stress appears to be close to zero. Stresses in the outer surface of thicker coatings are higher (more tensile) than in thinner coatings. Even when the average stress in the top coat is compressive, the stresses near the free surface of thick coatings are tensile. For thinner coatings the stresses near the free surface are possibly not high enough for initiation of the segmentation cracks.

The Young's modules of coating A, B, C, and D were determined by cantilever bending, with the free surface of the coating in tension. The results are presented in Fig. 15 as a function of segmentation crack density. The Young's modules are in the range of 4.5–10 GPa. Segmentation cracks are expected to have a strong influence on the Young's Modulus measured by this technique. Coating A, with the highest segmentation crack density, has the lowest Young's modulus. Due to the fact that segmentation cracks do not always penetrate entirely the thickness of the coating, lower values for the stiffness of the coating are expected when the free surface is loaded under tension. It is important to note that low values for the Young's modulus and yield strength of plasma spayed coatings have been reported before[9,23] and that they are beneficial for the behaviour in-service conditions of the TBCs as they indicate a higher compliance of the coating. Coatings with higher densities of segmentation cracks density perform better under thermal cycling.[4,5] Hence these microstructural features observed could be beneficial.

Even though the stress distribution along the thickness of the coatings appears similar for all samples, slight differences become evident when calculating the average residual stress after the deposition process. Fig. 16 shows that the average TC residual stress changes from tensile to compressive with increasing of average backsurface substrate temperature (it is worth noting that for typical temperatures

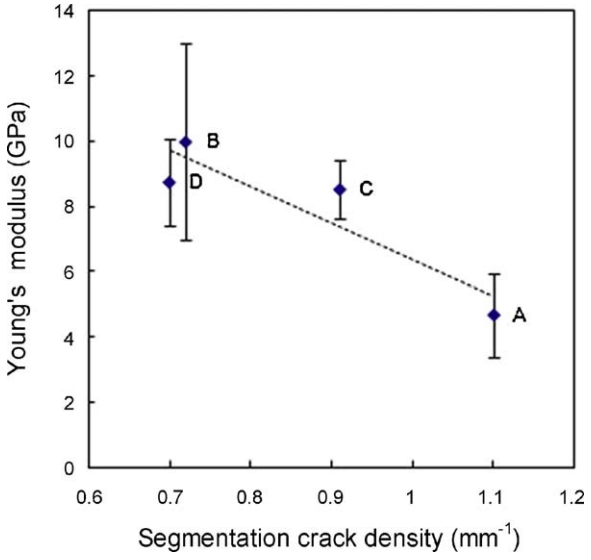

Fig. 15. Influence of segmentation crack density on Young's modulus of thick APS TBCs. Error bars indicate the standard deviation and the letters A, B, C, D refer to the corresponding coatings sprayed with conditions specified in the text.

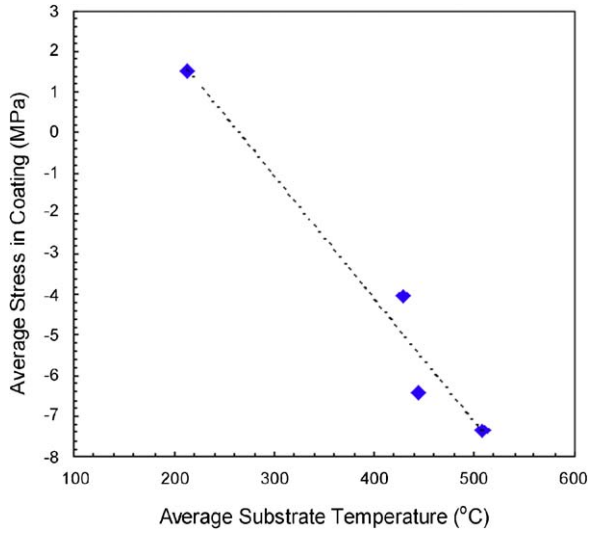

Fig. 16. Average residual stress in APS YPSZ top coat against average temperature at the substrate back surface during spraying.

experienced during coating deposition conditions the thermal conductivity for the mild steel substrate used in this study is similar to that of nickel superalloys, and hence no significant difference in the thermal histories of the substrates and the coatings are expected in both cases). There is a stress gradient through the thickness of the TC. It can be seen in Fig. 11 that stresses at the outer surface are tensile, with higher stresses (reaching 68 MPa) for the lower substrate temperature. At the TC/BC interface, stresses are compressive. Coatings deposited at higher temperatures showed the highest compressive stresses at the interface. With increasing substrate temperature, stresses become more compressive. The reason for this is that, as the substrate temperature is increased, the stresses due to differential thermal contraction generated on cooling increase, producing greater compressive residual stresses in the top coat. Similar results on the effect of substrate temperature on the residual stress state of the top coat have been reported.[14,24–26]

4. Conclusions

Thick thermal barrier coatings exhibit microstructural features, such as segmentation and branching cracks, which affect the elastic properties and which are not present in thinner TBCs. These cracks are generated as a result of relaxation of bi-axial tensile residual stresses near the free surface of thick TBCs. It is thought that segmentation cracks in TBCs will increase their compliance and hence their thermal shock resistance.

Crack segmentation density in thick thermal barrier coatings is strongly dependant on the substrate temperature during deposition. Higher average substrate deposition temperatures, combined with low variations between the minimum and maximum substrate temperature, give higher crack segmentation densities. Coatings with higher crack segmentation densities have a lower Young's modulus, which will contribute to higher thermal shock resistance. The average top coat residual stress changes from tensile to compressive with increasing average substrate temperature or with decreasing of the coatings thickness.

Acknowledgements

The author acknowledges the financial support received from Sulzer Metco, the Cambridge European Trust and from EPSRC for the realization of this work. There have been many useful discussions with industrial partners, particularly Jason Doesburg, Andrew Nicoll, Mitch Dorfman and Keith Harrison (Sulzer Metco). The authors would also like to like to thank Prof. T.W. Clyne and Kevin Roberts at the Department of Materials Science and Metallurgy, University of Cambridge.

References

1. Ahmaniemi S, Tuominen J, Vippola M, Vuoristo P, Mantyla T, Cernuschi F, Gualco C, Bonadei A, Di Maggio R. *J Therm Spray Technol* 2004;**13**(3):361.
2. Gualco GC, Campora A, Corcoruto S, Taylor R, Schwingel D, Oswald S.*Proceedings of United Thermal Spray Conference*. 1997.
3. Bengtsson P, Ericsson T, Wigren J. *J Therm Spray Technol* 1998;**7**(3):340.
4. Guo HB, Vassen R, Stover D. *Surf Coat Technol* 2005;**192**(1):48.
5. Schwingel D, Taylor R, Haubold T, Wigren J, Gualco C. *Surf Coat Technol* 1998;**108**(1–3):99.
6. Ahmaniemi S, Vuoristo P, Mantyla T, Cernuschi F, Lorenzoni L. *J Eur Ceram Soc* 2004;**24**(9):2669.
7. Ahmaniemi S, Vippola M, Vuoristo P, Mantyla T, Cernuschi F, Lutterotti L. *J Eur Ceram Soc* 2004;**24**(8):2247.
8. Tsipas SA, Golosnoy IO, Damani R, Clyne TW. *J Therm Spray Technol* 2004;**13**(3):370.
9. Thompson JA, Clyne TW. *Acta Mater* 2001;**49**(9):1565.
10. Gill SC, Clyne TW. *Metall Trans B* 1990;**21**(2):377.
11. Tsui YC, Clyne TW. *Thin Solid Films* 1997;**306**(1):23.
12. Tsui YC, Clyne TW. *Thin Solid Films* 1997;**306**(1):52.
13. Tsui YC, Peng XL, Clyne TW. In: Ericsson T, Oden M, Andersson A, editors. *5th International Conference on Residual Stresses*. Linkoping: Linkoping University Press; 1998. p. 442.
14. Bengtsson P, Johannesson T. *J Therm Spray Technol* 1995;**4/3**:245.
15. Sampath S, Jiang X. *Mater Sci Eng A* 2001;**304**:144.
16. Sampath S, Jiang XY, Matejicek J, Leger AC, Vardelle A. *Mater Sci Eng A* 1999;**272/1**:181.
17. Hutchinson JW, Suo Z. *Adv Appl Mech* 1992;**29**:63.
18. Guo HB, Vassen R, Stover D. *Surf Coat Technol* 2004;**186**(3):353.
19. Schwingel D, Taylor R, Wigren J. *High Temp-High Press* 1998;**30**(3):253.
20. Clyne TW. Residual Stresses in Surface Coatings and Their Effects on Interfacial Debonding, In: Clyne TW, editor. Interfacial Effects in Particulate, Fibrous and Layered Composite Materials, Key Eng Mater, vol. 116–117; 1996. pp. 307–330.
21. Clyne TW, Gill SC. *J Therm Spray Technol* 1996;**5**(4):401.
22. Apelian D, Paliwal M, Smith RW, Schilling WF. *Int Met Rev* 1983;**28**(5):271.
23. Choi SR, Zhu DM, Miller RA. *J Am Ceram Soc* 2005;**88/10**:2859.
24. Scardi P, Leoni M, Bertini L, Bertamini L. *Surf Coat Technol* 1997;**94–95**(1–3):82.
25. Takeuchi S, Ito M, Takeda K. *Surf Coat Technol* 1990;**43–44**(1–3):426.
26. Teixeira V, Andritschky M, Fischer W, Buchkremer HP, Stover D. *Surf Coat Technol* 1999;**120**:103.